Kinetic study of the oxidation by oxygen of liquid Al-Mg 5%alloys

Karine Surla, Françoise Valdivieso, Michèle Pijolat, Michel Soustelle, Marie-Agnès Prin-Lamaze

Kinetic study of the oxidation by oxygen of liquid Al-Mg 5%alloys

K. Surla (+§), F. Valdivieso (+), M. Pijolat (+*), M. Soustelle (+), M. Prin (§)
(+)Département ProcESS, Centre SPIN, Ecole Nationale Supérieure des Mines, 158 Cours Fauriel, 42023 Saint-Etienne Cedex2, FRANCE.
(§) Pechiney Centre de Recherches de Voreppe, Centr'Alp, BP 24, 38340 Voreppe, FRANCE.

(*) mpijolat@emse.fr

Abstract :
The oxidation into MgO of an industrial Al–Mg 5% alloy in the liquid state has been studied at 700°C by thermogravimetry, under controlled oxygen partial pressure. Since the kinetic curves were not reproducible, it was not possible to obtain directly from them the variations of the areic conversion rate (mol of MgO s^{-1} m^{-2}) versus the oxygen partial pressure. Therefore, it has been necessary to use a method based on the isolation method, which allowed us to overcome the problems of non-reproducibility of the curves. It was found that the areic rate of growth of MgO decreases when the oxygen pressure increases. A reaction mechanism in elementary steps has been proposed to account for these results, involving two competitive oxygen adsorptions on the MgO surface.

Keywords : *Al-Mg ; oxidation ; oxygen pressure ; kinetics ; Areic growth rate*

INTRODUCTION

Aluminium–magnesium alloys are widely used in industry (packaging, aerospace, transportation, building…).
During the manufacture of these alloys, the surface of the liquid metal may be oxidised, mainly leading to the formation of MgO, especially in the case of alloys containing more than 3% in magnesium [1 and 2]. To avoid this drawback, beryllium was added to the alloys in the past. Present knowledge of the potential hazards of this element leads most aluminium manufacturers to discard its use in spite of the very low level involved. In any case, it is planned to be forbidden soon. Thus, it is necessary to find alternative ways to prevent oxidation.
It is, therefore, important to understand the mechanisms involved in the formation of magnesium oxide from the alloy. The gaseous atmosphere involved in the industrial process is quite complex, since several gases can react with the alloys (oxygen, water vapour, nitrogen, carbon dioxide…).
So, we have studied a simplified system: the oxidation of an Al–Mg 5% alloy by oxygen. This article deals with an experimental study of the influence of the oxygen pressure on the oxidation, and an interpretation of the results in order to have a better knowledge of the reaction mechanism.
The transformation of a solid involves the processes of nucleation and growth of the new phase (MgO in our case). The experimental rate corresponds to the growth of MgO, thus, the modelling of the transformation is reduced to the growth model. It is simplified using the following assumptions:

(i) the system is in a quasi-steady state

(ii) the derivative of the fractional conversion α versus time, which will be also called the rate, can be written:

$$R = \frac{d\alpha}{dt} = \Phi.E \qquad [E.1]$$

where Φ is the areic growth rate of MgO (in mol s^{-1} m^{-2}), which depends on the physicochemical variables (pressure *P*, temperature *T*, magnesium activity...), and *E* is the 'space function' (m^2 mol^{-1}), characteristic of the extent of the area where the rate-limiting step of the growth occurs. *E* depends on the time and on the history of the solid from the beginning of the transformation up to the considered instant [3]. These two assumptions can be verified experimentally [3, 4 and 5].
Then, an experimental method, based on the isolation method [6], can be used to obtain directly the variations of Φ with the physico-chemical variables (particularly the oxygen pressure).
In this article, we present first the results of the kinetic study of the oxidation of an Al–Mg alloy into MgO; then a mechanism is proposed in order to account for the experimental results on the variations of the areic growth rate with oxygen pressure.

EXPERIMENTAL

The alloy is an industrial Al–Mg 5% alloy, supplied by Pechiney (purity about 99%). The samples are cylinders of 1 mm height and 9 mm diameter. Before each experiment, they were manually polished with grade 500 SiC paper and rinsed with acetone (the polishing method of the samples has no influence on the kinetic curves).
The oxidation of the liquid alloy was followed by isothermal thermogravimetry at 700°C (thermobalance SETARAM TAG 24). The experiments were carried out at atmospheric pressure, under a flowing mixture of helium and oxygen (1 l h^{-1}), the partial pressures being controlled by mass-flowmeters (Brooks 5850E).
The heating of the samples was carried out under oxygen at atmospheric pressure since it has been observed that a high oxygen pressure limits the oxidation of the liquid alloy; the oxygen pressure at 1 atm was first held for 30 min at 700°C. Subsequently, the oxygen pressure was changed to the value chosen for that particular experiment.
The experiments of simultaneous calorimetry and thermogravimetry were performed using a SETARAM TG-DSC 111, under a flowing mixture of helium and oxygen.
In situ IR study was carried out with a Spectra Tech cell (model 0030-13) and a spectrometer Biorad FTS 185, under a flowing mixture of argon and oxygen, using a magnesium powder (approximately cylindrical grains of length ranging between 400 and 500 μm).
Micrographs were obtained on a scanning electron microscope Jeol JSM 840.

RESULTS

Kinetic curves.

As shown in previous studies [7, 8, 9, 10, 11], for alloys containing more than 3% in magnesium, MgO is the first phase which appears during the oxidation. We present in Fig. 1 the results of thermodynamic calculations giving, at equilibrium, the oxygen pressure versus magnesium activity, for the alloy at 700°C. Fig. 1 indicates that MgO is the thermodynamically stable phase as long as the residual magnesium activity in the alloy is higher than 0.023, which corresponds to a weight increase of 1.7% (the calculation of theses values is detailed in Appendix A). After this limit, $MgAl_2O_4$ appears; we have confirmed its formation by X-ray diffraction, as reported previously [11]. Consequently, the kinetic curves will be limited to a weight increase of about 1.7%.
During the oxidation experiments, a thin solid MgO layer is formed when the temperature increases, and when the alloy melts, at about 648°C, it remains inside this solid layer which envelops the liquid metal. This layer undergoes strong deformations

during the experiments, it is very rough and irregular. It appears quite different from one experiment to another, as shown by the SEM micrographs of Fig. 2, which present the surface of two samples oxidised up to the same weight uptake (0.7%), in the same conditions of temperature and pressure (P_{O_2}=400 h Pa).
SEM observations have also shown that the oxide layer is formed of small MgO particles (about 0.5 μm) (Fig. 3a). Moreover, some holes are observed inside the samples, in which MgO parallelepipeds are located (10–15 μm) (Fig. 3b).
The experiments have been carried out with oxygen pressures ranging from 200 to 800 h Pa. The various kinetic curves have the shape given in Fig. 4 (corresponding to an oxygen pressure of 400 h Pa). The curves are very irregular and not reproducible, which is not surprising since the samples undergo very important morphological changes during the reaction, which differ from one experiment to another.

'Quasi-steady state' assumption

It can be shown [4] that when a system is in a quasi-steady state, there should be a parallel relationship between the curves of reaction rate versus time, obtained with two different experimental techniques, the axes being the rate axis and the direction the time axis.
We have chosen to measure simultaneously the oxidation rate by thermogravimetry and calorimetry (heat flow). The curves of rate of weight uptake and heat flow versus time have to be superimposed in two axis systems with different ordinate scales. Fig. 5 shows the curves obtained at 700°C for an oxygen pressure of 200 h Pa.
During the temperature increase (10°C/min), the alloy melting (at about 648°C) induces a strong endothermic signal, which hides the exothermic signal due to the oxidation up to about 80 min (or Δm=0.4%). Then, the curves are very well superimposed. Thus, the approximation of the quasi-steady state is valid at least from a weight uptake of 0.4%, i.e. a fractional conversion equal to 0.12 (the fractional conversion α is defined as: $\alpha = \frac{\Delta m(t)}{\Delta m_f}$, where $\Delta m(t)$ is the weight uptake at time t, and Δm_f is the weight uptake corresponding to the total consumption of the magnesium of the alloy, equal to 3.2% in our case).

'ΦE' assumption

In order to verify that the rate R can be written as in Eq. (E.1), we use the isolation method, which consists into changing suddenly a physico-chemical variable (P, T) from a value Y_0 to a value Y_1, at a given fractional conversion. Practically, we have changed the oxygen pressure from 400 to 200 h Pa, at various fractional conversions. Some experimental curves are given in Fig. 6, the pressure change being indicated by the horizontal arrows.
Let $R_{bi}(P_0, \alpha_i)$ and $R_{ai}(P_1, \alpha_i)$ be the rates before and after the pressure change at the fractional conversion α_i. They can be written (cf. Eq. (E.1)):
$R_{bi}(P_0, \alpha_i)=\Phi(P_0)E(\alpha_i)$ and $R_{ai}(P_1, \alpha_i)=\Phi(P_1)E(\alpha_i)$
so their ratio is:

$$\frac{R_{ai}(P_1,\alpha_i)}{R_{bi}(P_0,\alpha_i)} = \frac{\Phi(P_1)E(\alpha_i)}{\Phi(P_0)E(\alpha_i)} = \frac{\Phi(P_1)}{\Phi(P_0)} \qquad [E.2]$$

The ratio of the rates before and after the pressure change does not depend on the fractional conversion, thus, the '*ΦE*' assumption is verified if this ratio is constant, whatever the fractional conversion at which the pressure is changed.
The results are indicated in Fig. 7, which shows that two domains of weight uptake can be distinguished in which the '*ΦE*' test is verified. The rates ratio is approximately constant for a fractional conversion between 0 and 0.2 (weight uptake between 0.25%

and 0.6%), and then between 0.3 and 0.52 (weight uptake between 1% and 1.7%), but the ratio value is different in each domain.
The validity of the 'ΦE' test has also been verified by increasing the oxygen pressure from 200 to 400 h Pa, since Eq. (E.2) implies that the ratio $\frac{R(200\ h\ Pa)}{R(400\ h\ Pa)}$ should depend only on the two oxygen pressures, and not on the experimental method (starting pressure 200 or 400 h Pa). The values of the ratio obtained in both domains of weight gain by increasing the oxygen pressure from 200 to 400 h Pa are indicated by squares on Fig. 7. They are in very good agreement with the values obtained by decreasing the pressure from 400 to 200 h Pa, which proves that the 'ΦE' test is verified in both domains of weight uptake.
This conclusion has been confirmed with isobaric experiments in which the temperature has been changed from 700°C to 715°C.
Besides, it has been verified that when the experiments are repeated several times at a given fractional conversion, the value of the rates ratio is nearly the same (error less than 10%). Thus, the areic growth rate Φ (which is an intrinsic characteristic of MgO) is reproducible, the non-reproducibility of the kinetic curves (Fig. 4) coming from the irregular variations of the space function E.
Moreover, it must be noticed that the magnesium activity a_{Mg} in the alloy varies during the oxidation reaction, so the fact that the 'ΦE' test is verified implies that the ratio $\frac{R_{ai}}{R_{bi}}$ does not depend on a_{Mg} in each domain of weight uptake, thus, either Φ is independent on a_{Mg}, or Φ can be written as:

$$\Phi(T, P, a_{Mg}) = f(a_{Mg}) \,.\, g(P, T) \qquad [E.3]$$

i.e. a_{Mg} is a separable variable from the growth rate.

Variations of Φ with P_{O2} in each domain of weight uptake.

The experimental method to obtain the variations of Φ with P_{O2} is also based on the isolation method. In that case, several changes are carried out at a given fractional conversion α_i, from an oxygen pressure P_0 (here 200 h Pa) to various pressures P_i (the temperature being constant).
The ratio of the rates before and after the change, equal to $\frac{\Phi(P_i)}{\Phi(P_0)}$ according to Eq. (E.2), is proportional to the variations of Φ with P_{O2}, ($\Phi(P_0)$ keeping the same value in all the experiments).
The variations of Φ with P_{O2} were obtained by changing the oxygen pressure at a fractional conversion 0.15 in the first domain of weight uptake (Δm<0.6%) and at 0.4% in the second domain of weight uptake (1%<Δm<1.7%). Fig. 8a and b shows that in each domain, the areic growth rate decreases strongly when the oxygen pressure increases, which is quite unusual for oxidation reactions. As it can be seen, the higher the oxygen pressure, the slower the rate, which justifies our choice of heating the samples under an oxygen pressure of one atmosphere before establishing the oxidation conditions at 700°C.

INTERPRETATION OF THE VARIATIONS OF Φ WITH P_{O2} : GROWTH MECHANISM.

We have verified the assumption of quasi-steady state, and that the oxidation rate could be written as a product 'ΦE'. These results are important to find the elementary steps of

the growth mechanism, because they mean that it will be possible to use the assumption of the rate-limiting step to calculate the corresponding possible rate laws. Comparing these laws to the experimental variations of Φ with P_{O_2} (Fig. 8) will normally lead us to determine the rate-limiting step of the reaction and, thus, the appropriate rate law for Φ. Before detailing the elementary steps proposed for the reaction mechanism, a qualitative description can be attempted.
Usually, the mechanisms proposed to describe the oxidation of metals lead to a areic growth rate Φ which increases when the oxygen pressure increases [11, 12, 13 and 14]. Nevertheless, studying the oxidation of solid magnesium into MgO [11 and 12], we have obtained complex variations of the growth rate Φ with the oxygen pressure, the curve Φ(PO2) passing through a maximum. We have succeeded in interpreting these results considering a growth mechanism which involves two kinds of oxygen adsorption on the MgO surface [12].
In the case of the alloy, we can also make this assumption to account for the inhibiting effect of oxygen on the growth rate of MgO, since it is well known that oxygen adsorption on the surface of an oxide may lead to various oxygen species [15]. In the case of magnesium oxide, several adsorbed species of oxygen have already been observed [16 and 17], like O^- and O_2^-. To confirm the existence of such species at the MgO surface in the experimental conditions used for the Al–Mg 5% oxidation experiments, we have carried out in situ infra-red experiments during the oxidation of solid magnesium. The IR spectra, obtained from 25°C to 500°C, are given in Fig. 9. It can be seen that when the temperature increases (and MgO is formed), a band at 1016 cm−1 appears, which can be attributed to O2− species, according to [18], and to the literature data on other oxides such as CeO2 [19 and 20].
These O2− species are very stable, since the band at 1016 cm−1 is not modified at 500°C even when oxygen is removed from the gaseous atmosphere. This is in agreement with a thermodesorption study showing that there exists oxygen species adsorbed on the MgO surface which desorb at temperatures as high as 880°C []. These species are supposed to be inactive for the oxidation reaction, and to occupy adsorption sites. A competitive oxygen adsorption is assumed to occur on the same sites, leading to oxygen adsorbed species which participate in the oxidation. These two kinds of adsorbed species can be described as shown in Fig. 10. Some oxygen species may be adsorbed on a surface site (which could be a magnesium atom at the MgO surface), perpendicularly to the surface (scheme (a) in Fig. 10). The second kind of adsorbed species are parallel to the surface, the adsorption involving four surface sites (scheme (b) on Fig. 10). The choice of four sites will be discussed later.
In the following, ‘s’ designates a surface site, which could be a magnesium atom at the MgO surface. The steps proposed for the reaction mechanism are detailed below:

a non dissociative adsorption:

$O_2 + s \Leftrightarrow O_2\text{-}s$

This adsorption is considered to be at equilibrium (equilibrium constant KA) and the O2−s species do not participate in the oxidation.

a dissociative adsorption, in two steps, involving four sites ‘s’:

$O_2 + 4s \Leftrightarrow O_2\text{-}s_4$ (1a)

$O_2\text{-}s_4 \Leftrightarrow 2\ O\text{-}s + 2s$

Then, the following steps involve the MgO point defects (magnesium vacancies and holes):

* step (2) : external interface reaction (creation of the oxide defects)

$$O - s \Leftrightarrow O_o + V''_{Mg} + 2h^{\bullet} + s \qquad (2)$$

* step (3) : diffusion of the defects from the external interface to the internal interface

* step (4) : internal interface reaction

$$Mg_{alloy} + V''_{Mg} + 2h^{\bullet} \Leftrightarrow Mg_{Mg_{oxide}} \qquad (4)$$

A linear combination of steps (1a), (1b) and (2), (3) and step (4) leads to the overall reaction: $Mg+1/2O_2=MgO$.
The rate laws have been calculated using the assumption of the rate-limiting step A linear combination of (1a), (1b) and (2), (3) and step (4) leads to the overall reaction: $Mg+1/2O_2=MgO$.
The rate laws have been calculated using the assumption of the rate-limiting step [4]. Only the cases for which the steps of adsorption (Eq. (1a), dissociation (Eq. (1b) or external interface (Eq. (2) are rate-limiting lead to rate laws which can account for a decreasing rate when the oxygen pressure increases. They are indicated in Table 1.
It can be noticed that the variation of Φ with P_{O_2} being the same in (1a) and (1b), it will not be possible to choose between these two possibilities.
The experimental values were fitted using the functions given in Table 1. The results obtained for the first domain of weight uptake are shown in Fig. 11a and b, in (1a), (1b) and (2), respectively.
The function corresponding to the rate-limiting (1a) and (1b) leads to a good agreement with the experimental values, as shown by the correlation factor equal to 0.99 (Fig. 11a). It is also the case in the second domain of weight uptake ($\Delta m>1\%$), the correlation factor being 0.97 (Fig. 12a). Step (2) is not so satisfactory (Fig. 12b). Step (1a) was assumed first to involve two adsorption sites instead of four, but the agreement was not as satisfactory as with four sites.The rate law depends on the magnesium activity a_{Mg}, but the fit with the experimental values leads to a value of $\frac{1}{K_2 K_4 a_{Mg}}$ of 2.2×10^{-2}, which is low compared to 1 and to $K_A P_{O_2}$ and, thus, Φ can be considered as independent of a_{Mg}. This is compatible with the fact that the 'ΦE' test is verified (cf. Section 3).
The term $\frac{1}{K_2 K_4 a_{Mg}}$ being neglected in the expression of the rate law, K_A (the equilibrium constant of the non-dissociative adsorption) is the only parameter to be adjusted, since in the ratios $\frac{\Phi(P)}{\Phi(P_0)}$ the rate constant (k_{1a} or k_{1b}) is eliminated. For the first and second domain of weight uptake, we obtain K_A=7.9 and 29, respectively.
Thus, the existence of the two domains of weight uptake is linked to a change in the equilibrium constant K_A. Taking into account the two kinds of morphologies of magnesium oxide which have been observed (small grains and parallelepipeds), the two values of K_A may correspond to the oxygen adsorption on each oxide type. Thus, each domain of weight uptake is attributed to a predominant morphology.
Concerning the rate-limiting step, we can not conclude whether or not it is different from one domain to another (the rate laws ((1a) and (1b)) being the same).

CONCLUSIONS

The oxidation kinetics of a liquid industrial Al–Mg 5% alloy has been studied in an attempt to validate a reaction mechanism. The use of the isolation method turned out to be necessary to overcome the problems due to the non-reproducibility of the kinetic curves and to obtain the variations of the areic growth rate of magnesium oxide Φ with the oxygen pressure.

It has been shown that Φ decreases when oxygen pressure increases, which was accounted for by a mechanism involving two parallel oxygen adsorptions, one is non-dissociative, the other is dissociative on four adsorption sites and participates in the oxidation. Moreover, evidence for two domains of weight uptake has been found, in which the growth rate Φ is different, although the rate-limiting step seems to be the same. The origin of these two domains could not be identified with certainty, but SEM observations showing that the oxide exists in two different morphologies, and the suggested mechanism leading to distinct values of the equilibrium constant of oxygen adsorption K_A in the two domains of weight uptake, each domain could correspond to a predominant oxide morphology.

Finally, it would be interesting to determine whether the transition between the two domains (for a fractional conversion ranging from 0.2 to 0.3 for an alloy containing initially 5% in magnesium) corresponds to the formation of a given amount of magnesium oxide or to a residual magnesium content in the alloy. This could be done in a further study by using alloys with various contents of magnesium, and could lead to a better understanding of the origin of these two domains.

ACKNOWLEDGEMENTS

This work has been carried out in the frame of a CPR (Contrat de Programme de Recherches): 'REACTIVITE des ALLIAGES LIQUIDES à HAUTE TEMPERATURE et RECYCLAGE': Contrat de Programme de Recherches between CNRS, INP Grenoble, INP Lorraine, INP Toulouse, the Ecole nationale supérieure des mines de Saint-Etienne and PECHINEY RECHERCHE.

Appendix A. Determination of the domains of stability of MgO and $MgAl_2O_4$

In the system (Al, Mg, O_2), three reactions can occur:

$$2Mg+O_2=2MgO \quad (1)$$

$$Mg+2Al+2O_2=MgAl_2O_4 \quad (2)$$

$$2Al+3/2O_2=Al_2O_3 \quad (3)$$

The corresponding Gibbs energies are:

$$\Delta G_1=\Delta G_1^0-RT\ln a_{Mg}{}^2 P_{O_2} \quad (Eq.1)$$

$$\Delta G_2=\Delta G_2^0-RT\ln a_{Mg} a_{Al}{}^2 P_{O_2}{}^2 \quad (Eq.2)$$

$$\Delta G_3=\Delta G_3^0-RT\ln a_{Mg} a_{Al}{}^2 P_{O_2}{}^{3/2} \quad (Eq.3)$$

where ΔG_i^0 is the standard Gibbs energy of the equilibrium (i), given by thermodynamic tables [22], a_{Mg} and a_{Al} are the activities of magnesium and aluminium, respectively, in the alloy.

At equilibrium, the Gibbs energies ΔG_1, ΔG_2 and ΔG_3 are equal to zero, so we obtain for each of the three equilibria the variations of $\ln(P_{O_2})$ versus the magnesium activity a_{Mg}, presented in Fig. 1.

The boundary between the domains of stability of MgO and $MgAl_2O_4$ is determined by the intersection of the curves $\ln(P_{O_2})=f(a_{Mg})$ corresponding to (1) and (2):

$$\ln P_{O_2} = \frac{\Delta G_1^0(P)}{RT} - \ln_{Mg}^2 = \frac{\Delta G_2^0(P)}{2RT} - \frac{1}{2}\ln a_{Mg} - \ln a_{Al} \quad \text{(Eq.4)}$$

The Al–Mg alloys containing up to 12 at.% of magnesium exhibit a small deviation from the ideal behaviour [23 and 24]. The magnesium activity is given at 700°C by the relation []:

$$a_{Mg}=0.84x_{Mg} \quad \text{(Eq.5)}$$

where x_{Mg} is the atomic fraction of magnesium in the alloy.
The ideal solution behaviour is closely followed for aluminum. The activity coefficient of aluminum is nearly equal to one and, thus:

$$a_{Al}\approx x_{Al}. \quad \text{(Eq.6)}$$

From (Eq.4), (Eq.5) and (Eq.6), we obtain the expression giving the atomic fraction of magnesium remaining in the alloy above which $MgAl_2O_4$ is the stable phase:

$$\ln \frac{(084\chi_{Mg})}{(1-\chi_{Mg})^{2/3}} = \exp(\frac{2}{3}\frac{\Delta G_1^0}{RT} - \frac{\Delta G_2^0}{3RT}) \quad \text{(Eq.7)}$$

It comes: x_{Mg}=0.027, and then Eq. (Eq.5) leads to a_{Mg}=0.023.
This corresponds to a magnesium content of 2.43% in weight in the alloy. The corresponding percentage of weight uptake Δm (%) is given by the relation:

$$\Delta m(\%) = \frac{wt.\%ofMgconsumed}{M_{Mg}} M_0 = \frac{initial\ \ content\ \ of\ \ Mg(wt.\%) - 2.43\%}{M_{Mg}} - M_0$$

where M_{Mg} and M_O are the molar weights of magnesium and oxygen, respectively. For the Al–5% Mg alloy (containing 5% in weight of magnesium initially), we obtain: Δm(%)=1.7%.

REFERENCES

1. D.J. Field, Treatise on Materials Science and Technology, Ed. Doherty, 31, 523, (1989).
2. M.V. Malcev, J.D. Cistajakov and M.I. Cypin Dokl. Akad. Nauk. SSSR XCIX 5 (1954), p. 813.
3. M. Soustelle and M. Pijolat, Solid State Ionics, 95, 33, (1997).
4. K. Surla, Oxydation d'un alliage aluminium-magnésium à l'état liquide. Méthodologie de détermination de mécanismes réactionnels à partir d'expériences non nécessairement reproductibles, Thesis, Saint-Etienne, (1998).
5. J.P. Viricelle, M. Pijolat and M. Soustelle J. Chem. Soc., Faraday Trans. 91 24 (1995), p. 4437.
6. B. Delmon, in Introduction à la Cinétique Hétérogène, Ed. Technip, Paris, (1969).
7. W.W. Smeltzer J. Electrochem. Soc. 105 2 (1958), p. 67.
8. C.N. Cochran, D.L. Belitskus and D.L. Kinosz Metall. Trans. B 8B (1977), p. 323.
9. T. DebRoy, A. Bandopadhyay, R. Roy, J. Amer. Cer. Soc., 77 (5), 1296, (1994).
10. H. Venugolapan, K. Tankala and T. DebRoy, Mat. Sci. Eng., A210, 64, (1996).
11. K. Surla, F. Valdivieso, M. Pijolat, M. Prin, Récents Progrès en Génie des Procédés, 55 (11), 87, (1997).
12 K. Surla, F. Valdivieso, M. Pijolat, M. Soustelle and M. Prin Ann. Chim. Sci. Mater. 25 (2000), p. 601.
13. M. Caillet, Recherches sur la cinétique d'oxydation des poudres métalliques, Thesis, Grenoble, (1963).
14. P. Sarrazin, J. Besson, Métallurgie, VI, 11 (1966).
15. M. Che, A.J. Tench, Advances in catalysis, Academic press, 32, 130, (1983).
16. C. Naccache, H. Che, Catalysis, Highwater editor, Vol.2, 1389, (1973).
17. C.T. Au and M.W. Roberts J. Chem. Soc., Faraday Trans. 83 (1987), p. 2047.
18. J.C. Lavalley, personal communication.
19. C. Li, K. Domen, K. Maruya and T. Onishi J. Am. Ceram. Soc. 111 (1989), p. 7683.
20. J. Soria and A. Martinez-Arias J. Chem. Soc., Faraday Trans. 91 11 (1995), p. 1669.
21. H. Dunski, M. Sugier, Phys. Stat. Sol., K49, 113, (1983).
22. I. Barin , Thermochemical data of pure substances. Verlagsgesellschaft (1989).
23. B.L. Tiwari Metall. Trans. A 18A (1987), p. 1645.
24. Z. Moser, W. Zakulski, H. Rzyman, W. Gasior, Z. Panek *et al.* J. Phase Equilib. 19 1 (1998), p. 38.

FIGURE CAPTIONS

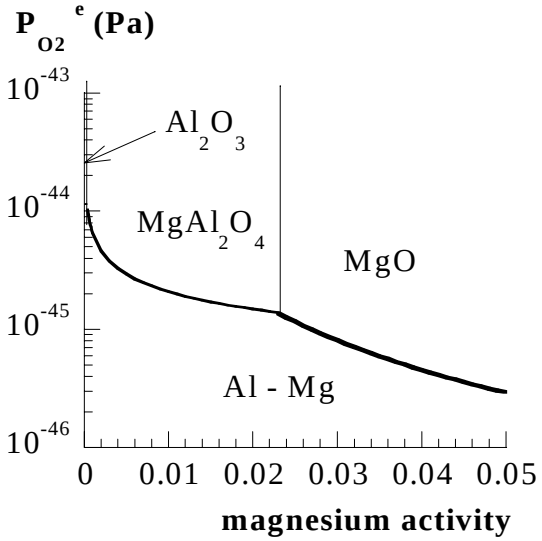

Figure 1: Thermodynamic stability of MgO, $MgAl_2O_4$ and Al_2O_3 phases. Oxygen pressure at equilibrium versus magnesium activity at 700°C.

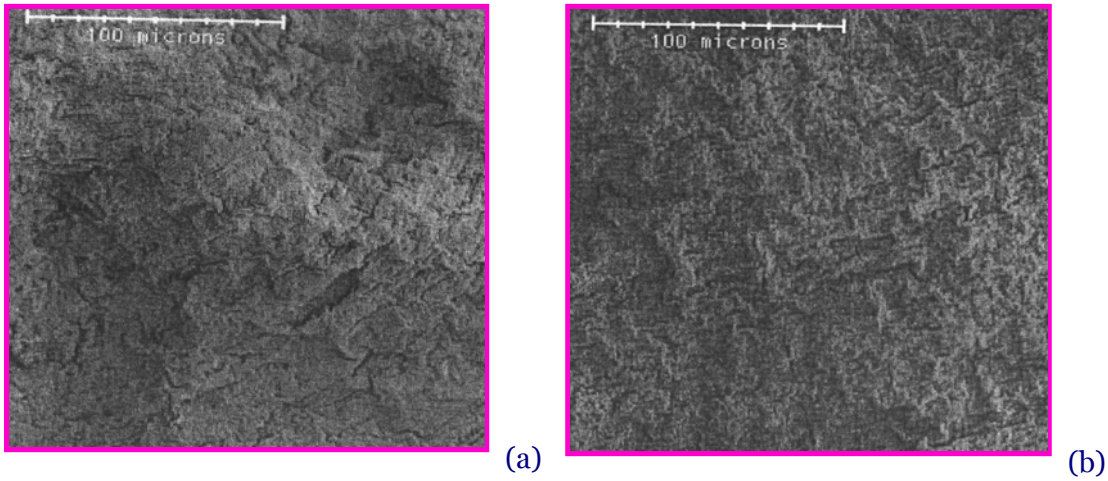

(a) (b)

Figure 2: Surface morphology of two samples oxidised up to a weight uptake of 0.7% (T=700°C, P_{O2} = 400 hPa)

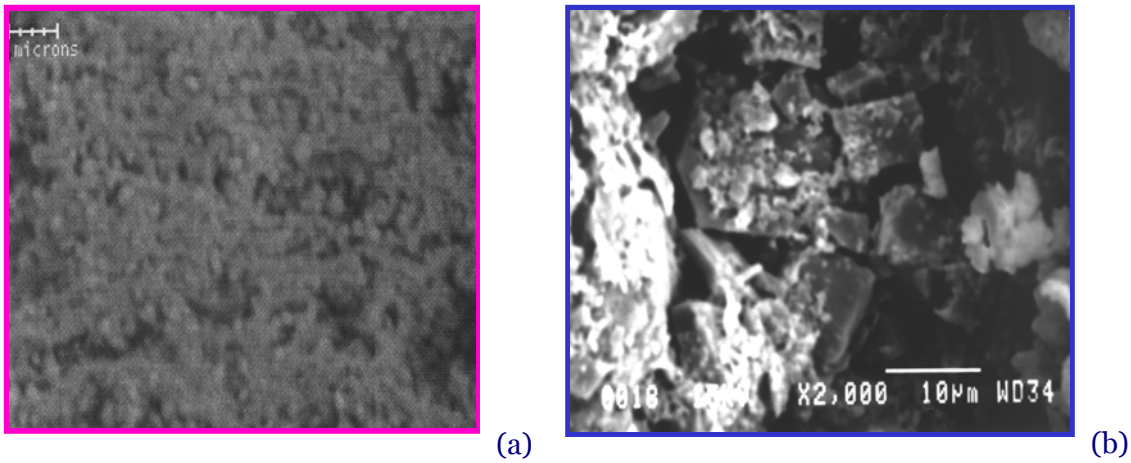

(a) (b)

Figure 3: Morphology of the MgO oxide issued from the oxidation of Al-Mg 5% alloy : surface of the samples (a) and in the holes (b).

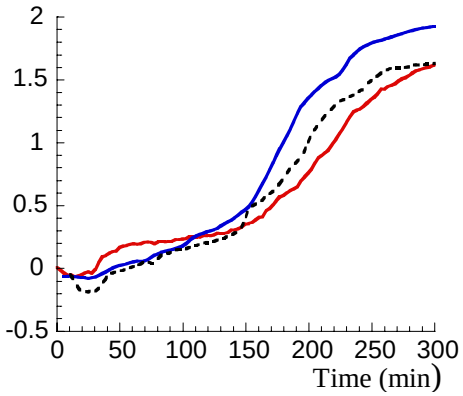

Figure 4: Curves of weight uptake and non-reproducibility (T=700°C, P_{O_2}=400hPa).

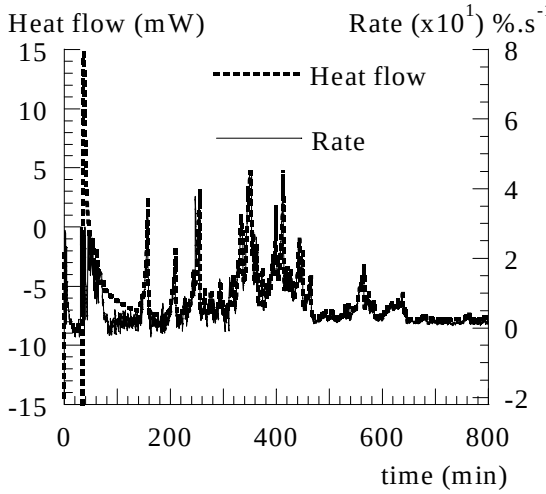

Figure 5: Quasi-steady state test (700°C, P_{O_2}=200 hPa).

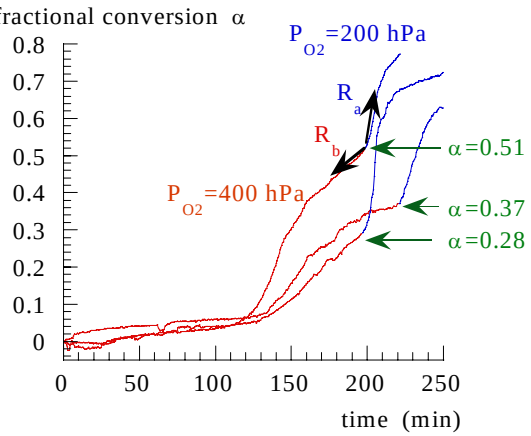

Figure 6: Application of the isolation method to the « Φ.E » test : oxygen pressure changes at various fractional conversions.

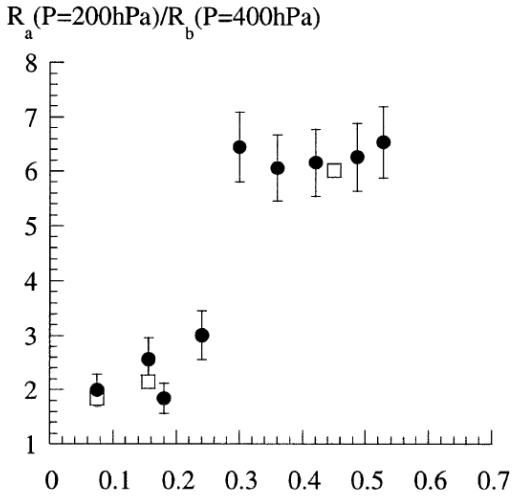

Figure 7: « Φ.E » test by changing the oxygen pressure from 400hPa to 200hPa and from 200 to 400 h Pa (squares).

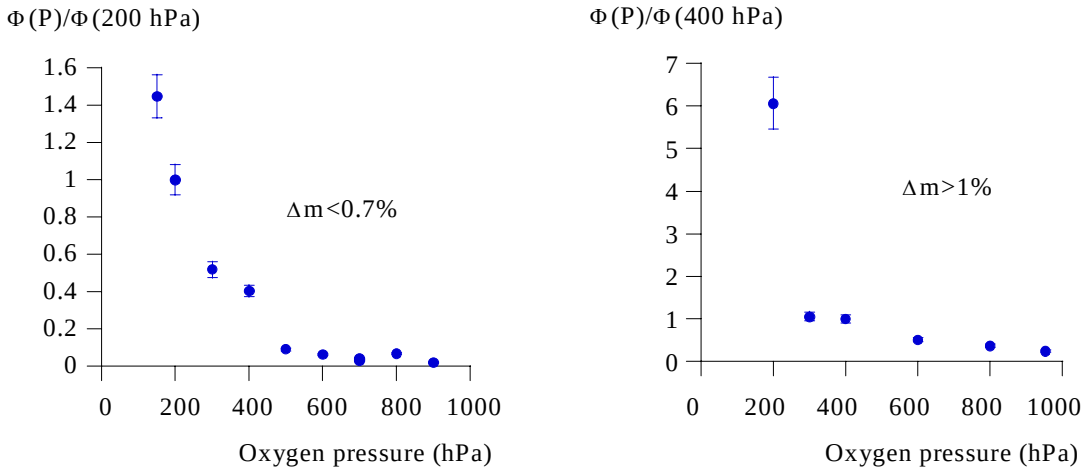

Figure 8: Variations of the areic growth rate Φ with oxygen pressure in each domain of weight uptake : Δm<0.6% (a) and Δm>1% (b).

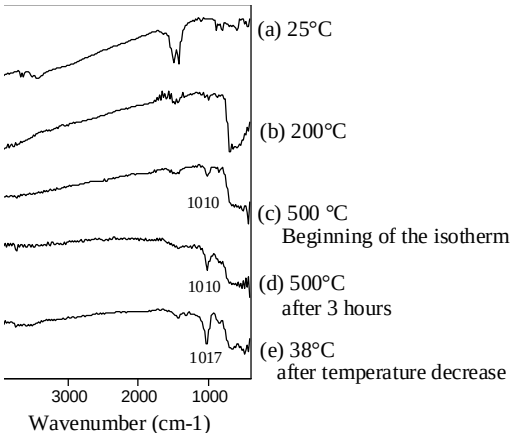

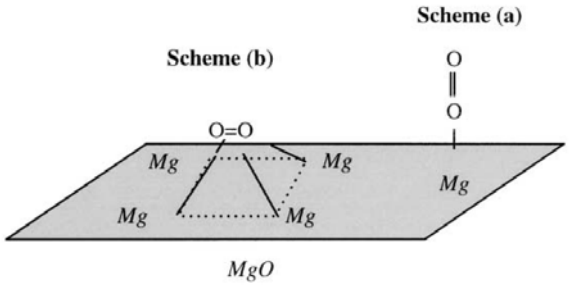

Figure 9: In-situ IR spectra recorded during the oxidation of solid magnesium at 500°C by oxygen.

Figure 10: Schematic representation of the two kinds of adsorbed oxygen species on the MgO surface.

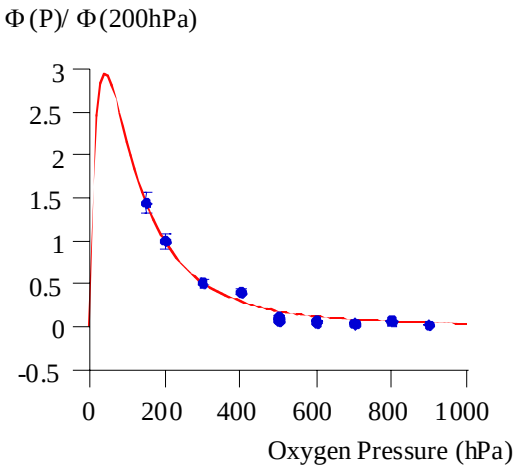

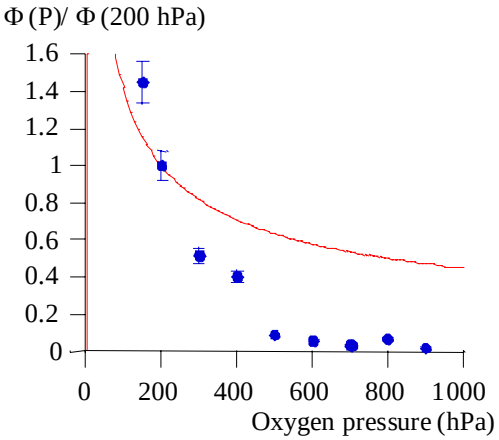

First domain: Δm<0,6%
Rate limiting step: (1a) or (1b)

Δm<0,6%
Rate limiting step: (2)

Figure 11: Fit between the experimental values and the theoretical rate laws in the first domain of weight uptake : (a) : rate laws (Eqs.(1a) or (1b), and (b) : rate law (Eq.(2)).

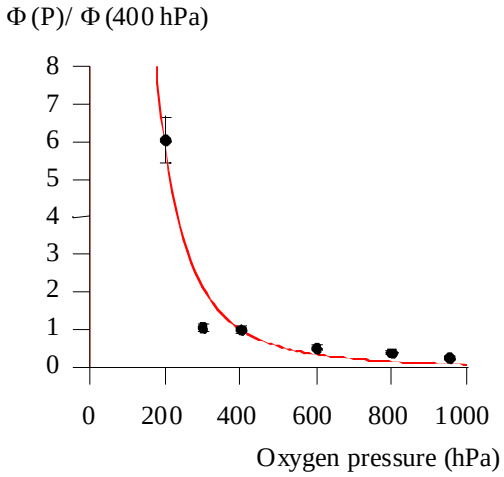

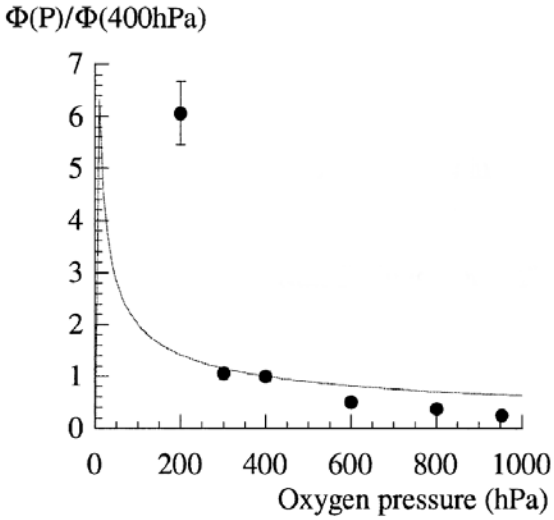

First domain: Δm>1%
Rate limiting step: (1a) or (1b)

First domain: Δm>1%
Rate limiting step: (2)

Figure 12: Fit between the experimental values and the theoretical rate laws in the second domain of weight uptake: (a) rate laws ((1a) and (1b)), and (b) rate law (Eq. (2).

TABLE CAPTION

Table 1 : Rate laws corresponding to the rate-limiting steps (1a), (1b) and (2) (k_i and K_j are respectively the rate constants and the equilibrium constants of the steps (i) and (j)).

Rate-limiting step	Areic growth reactivity
Adsorption (Eq.(1a))	$\Phi = k_{1a} \dfrac{P_{O_2}}{\left(1 + \dfrac{1}{K_2 K_4 a_{Mg}} + K_A P_{O_2}\right)^4}$
Dissociation of O_2-s_4 (Eq.(1b))	$\Phi = k_{1b} \dfrac{K_{1a}\ P_{O_2}}{\left(1 + \dfrac{1}{K_2 K_4 a_{Mg}} + K_A P_{O_2}\right)^4}$
Eexternal interface reaction (Eq.(2))	$\Phi = k_2 \dfrac{\sqrt{K_1 P_{O_2}}}{1 + \sqrt{K_1 P_{O_2}} + K_A P_{O_2}}$